Automated quantitative analysis of void morphology evolution in Ag-Ag direct bonding interface after accelerated aging

32th European Symposium on Reliability of Electron Devices, Failure Physics and Analysis

ESREF 2021

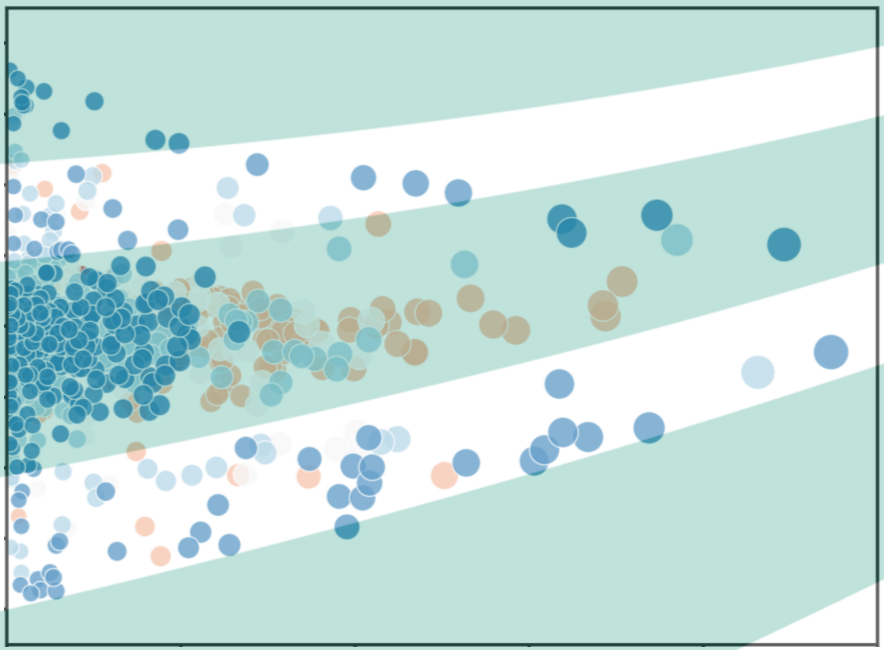

Z. Yu[a,b], T. Xu[a], S. Letz[a,b], C. F. Bayer[a], A. Schletz[a], M. März[a,b]

[a] *Fraunhofer IISB, Schottkystrasse 10, 91058 Erlangen, Germany*

[b] *Friedrich-Alexander University Erlangen-Nuremberg, Cauerstr. 9, 91058 Erlangen, Germany*

Fraunhofer IISB

Agenda

- **Motivation**
- Materials and Methods
  - Sample Preparation
  - Automated SEM and void analysis
- Results
  - Cross-section SEM micrographs
  - Individual and total void analysis
- Discussion
- Conclusion and Outlook

ESREF 2021

Fraunhofer IISB

Motivation

@ Fraunhofer IISB

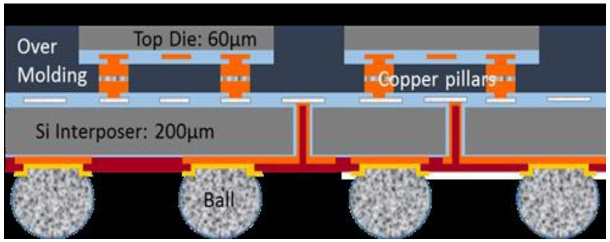

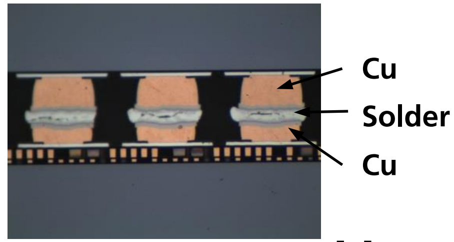

[1]

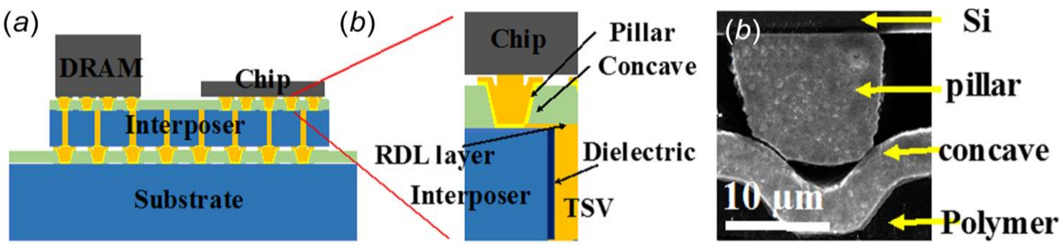

[2]

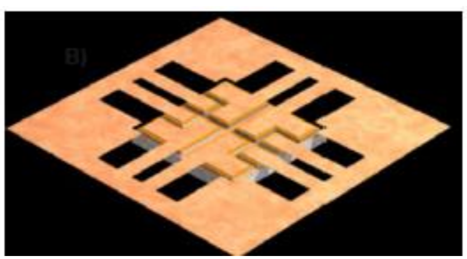

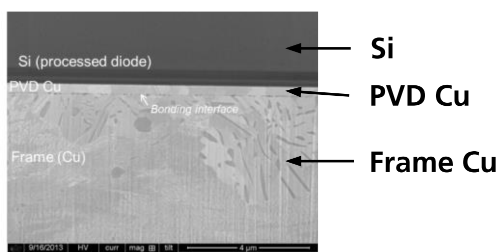

[3]

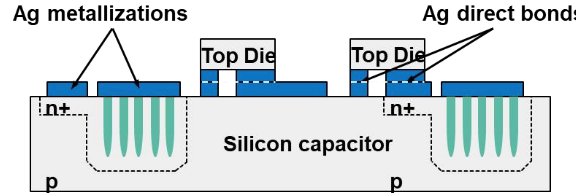

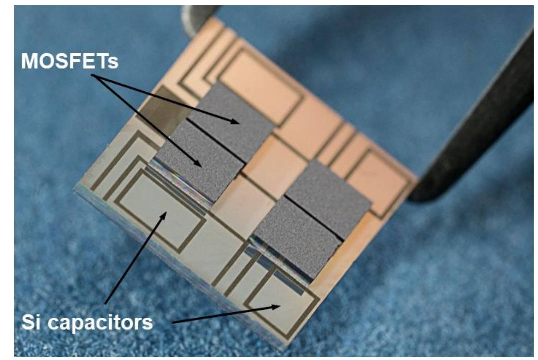

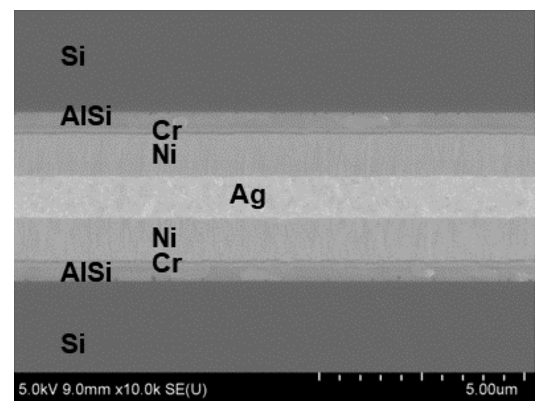

ESREF 2021

Fraunhofer IISB

Motivation

Introduction to Ag-Ag Direct Bonding

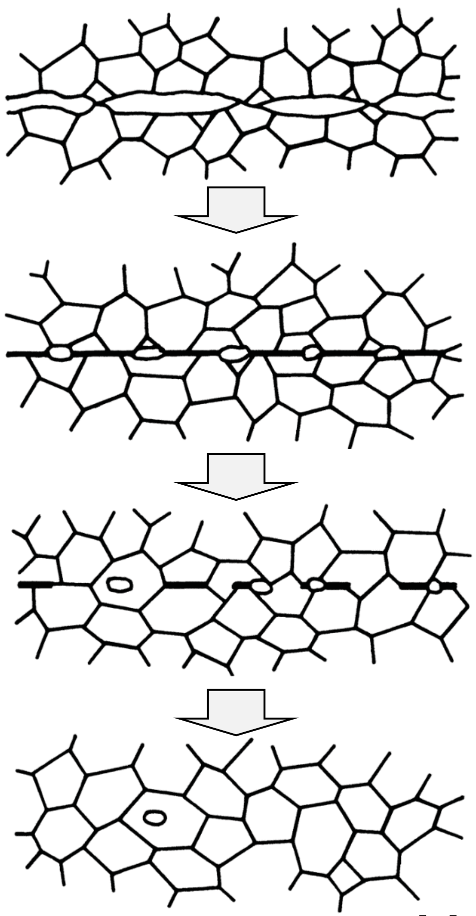

[4]

I. Initial asperity contact

II. Plastic deformation and interfacial boundary formation

III. Grain boundary migration and pore elimination

IV. Volume diffusion and pore elimation

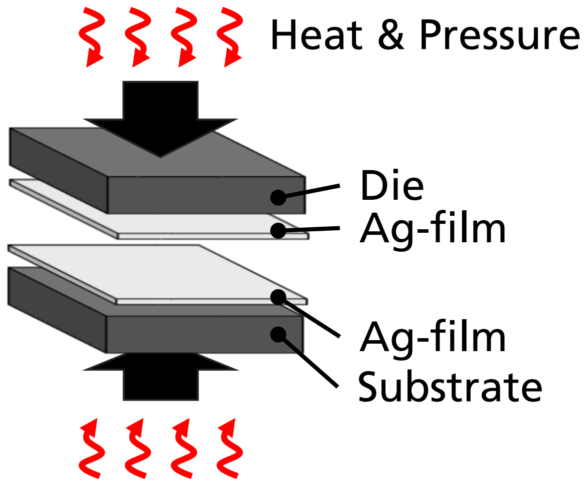

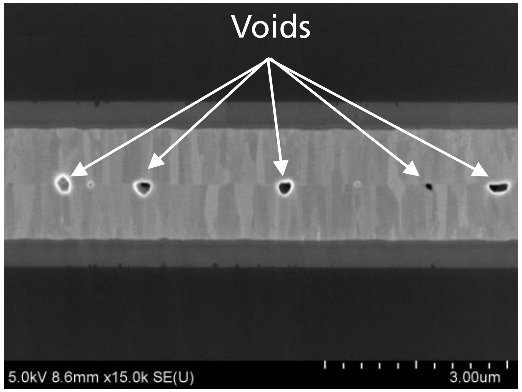

ESREF 2021

Fraunhofer IISB

Motivation

- Diffusion and deformation mechanisms occurring **during bonding** according to Hill and Wallach[5]:
  1. plastic yielding deforming an original contacting asperity.
  2. surface diffusion from a surface source to a neck;
  3. volume diffusion from a surface source to a neck;
  4. evaporation from a surface source to condensation at a neck;
  5. grain boundary diffusion from an interfacial source to a neck;
  6. volume diffusion from an interfacial source to a neck;
  7. power-law creep.

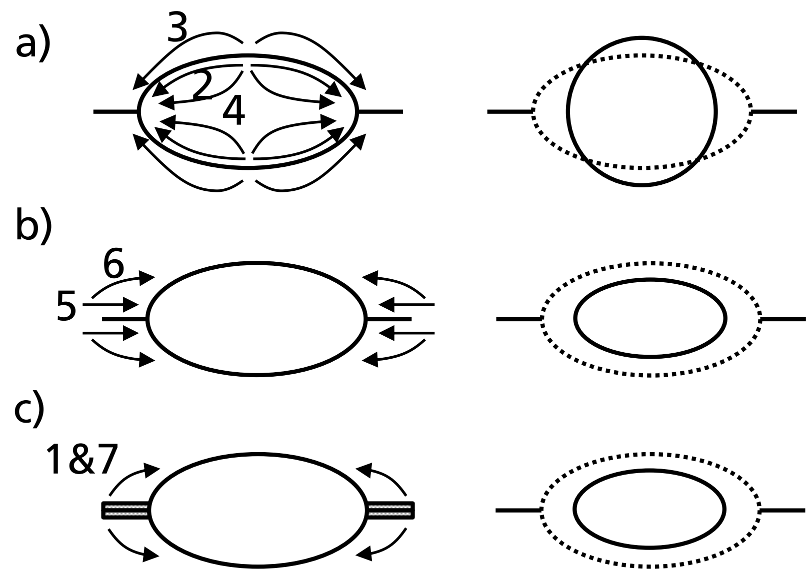

- **During reliability testing**
  - Routes of material transfer?
  - Void morphology evolution?

ESREF 2021
Fraunhofer IISB

Motivation

- What has changed in the void morphology from A to B?
  - Distribution?
  - Shape?
  - Size?
  - Count?
- **Quantitative analysis?**
  - SEM image processing
  - SEM image analysis
  - Data analysis
  - Data representation

  →Tracking and statistical analysis of void morphology evolution during accelerated aging

Initial after bonding

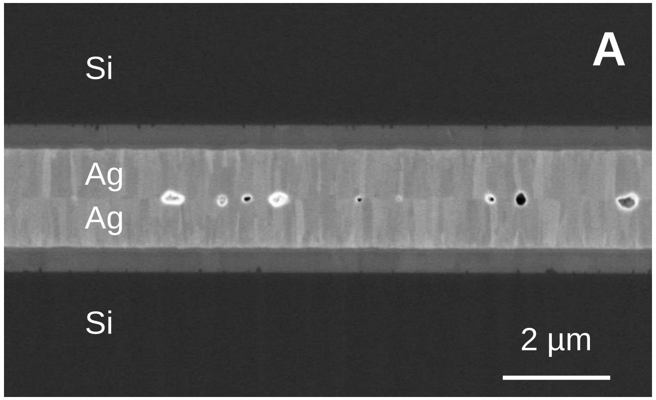

After Temperature Shock Test

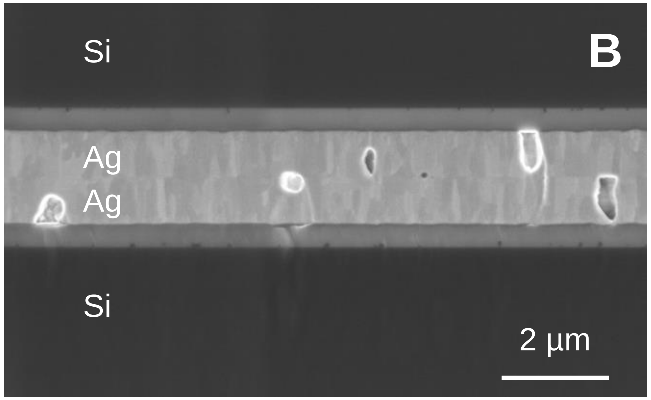

ESREF 2021
Fraunhofer IISB

Agenda

- Motivation
- **Materials and Methods**
  - Sample Preparation
  - Automated SEM and void analysis
- Results
  - Cross-section SEM micrographs
  - Individual and total void analysis
- Discussion
- Conclusion and Outlook

Materials and Methods

Sample Preparation

- Ag-Ag direct bonding in hot uniaxial-press
  - Temperature: 260 °C
  - Time: 10 min
  - Pressure: 20 MPa
- Temperature shock test (TST)
  - T_{max}: 220°C
  - T_{min}: -55°C
  - Dwell: 15 min
  - Cycles: 0/250/500/1000/2000
- Cross-section preparation with ion milling polishing system
- SEM observation and analysis

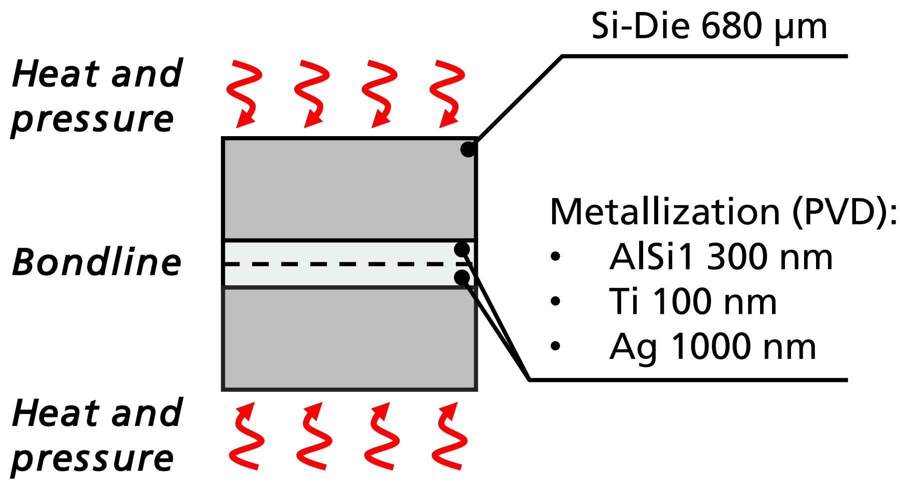

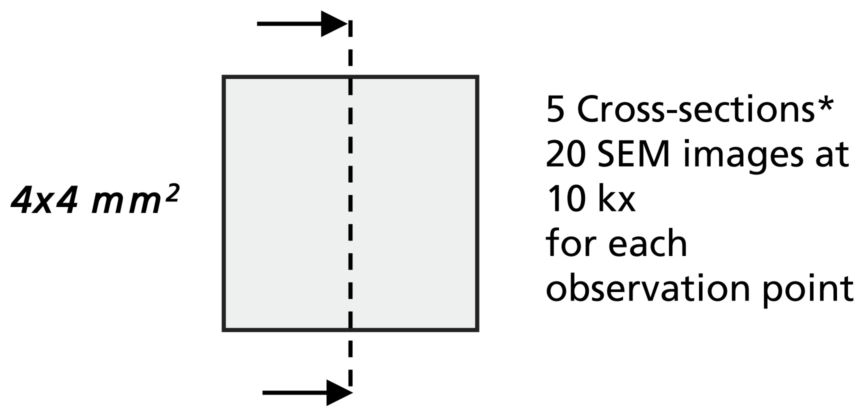

Material and Methods

SEM Analysis – Work flow

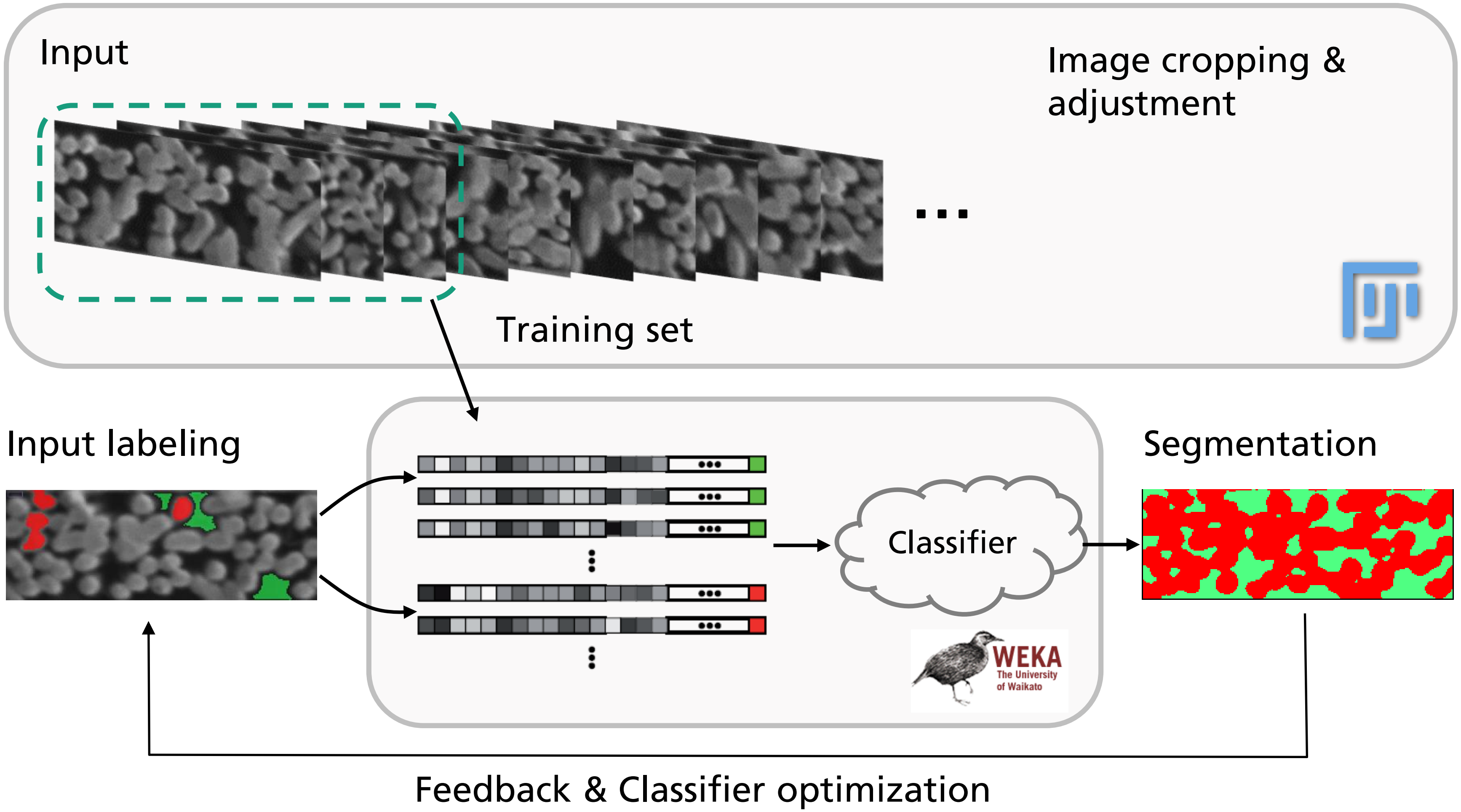

[6-7]

Material and Methods

SEM Analysis – Work flow

A

B

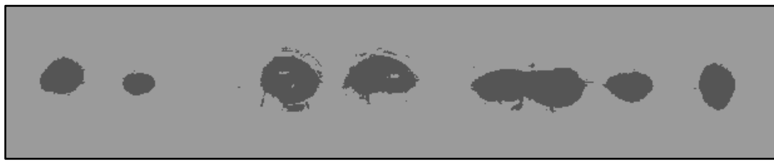

C

D

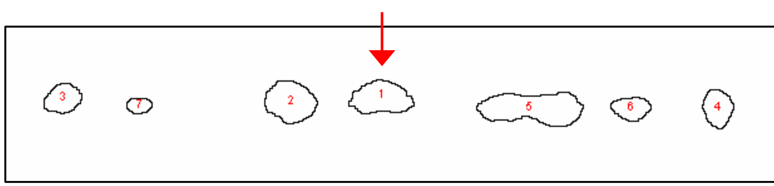

E

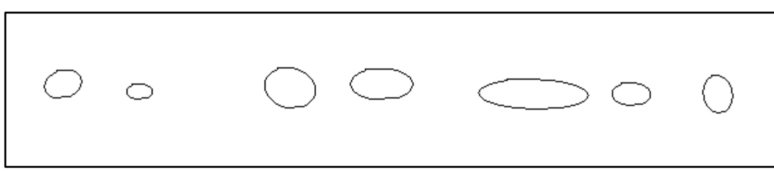

Trainable Weka Segmentation

Threshold & Binary

Analyze Particles

- Draw Outlines

- Fit Ellipse

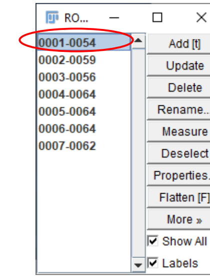

Results

File Edit Font Results

	Label	Area	Perim.	Major	Minor	Angle	Circ.	AR	Round
1	Classified image	0.096	1.323	0.487	0.252	179.592	0.692	1.932	0.518
2	Classified image	0.101	1.209	0.405	0.317	165.332	0.867	1.276	0.784
3	Classified image	0.051	0.861	0.297	0.220	19.595	0.870	1.350	0.741
4	Classified image	0.054	0.889	0.300	0.228	98.600	0.857	1.316	0.760
5	Classified image	0.160	2.014	0.863	0.237	178.598	0.497	3.643	0.275
6	Classified image	0.043	0.819	0.304	0.180	179.008	0.807	1.684	0.594
7	Classified image	0.019	0.518	0.201	0.122	1.749	0.906	1.647	0.607

Summary_a294_sample02.csv

File Edit Font

Slice	Count	Total Area	Average Size	%Area	Perim.	Major	Minor	Angle	Circ.
Classified image	7	0.525	0.075	7.141	1.090	0.408	0.222	117.496	0.785

Set Measurements

- Area
- Perimeter
- Major & Minor
- Circularity
- Etc.

Output Results & Summary

ESREF 2021

Fraunhofer IISB

Material and Methods
SEM Analysis – Objectives

- Individual Void Analysis
  - Distribution
  - Size (Area)
  - Shape (Aspect Ratio (major: minor axis))
- Total Void Analysis
  - Total area (%)
  - Counts per SEM image
  - Bonding ratio

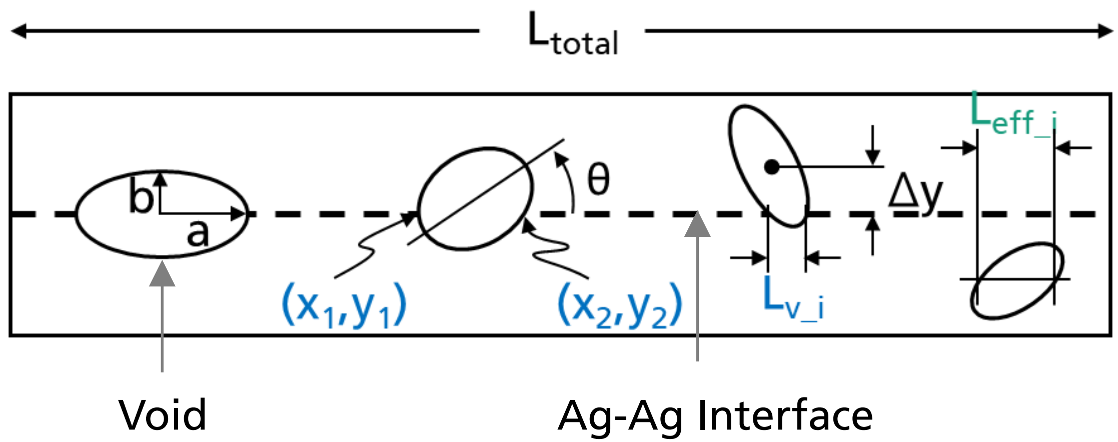

$$\textbf{Bonding ratio}\ (\%) = \frac{L_{total} - \sum_{i=1}^{n} L_{v\_i}}{L_{total}}$$

$$\textbf{Bonding ratio eff}\ (\%) = \frac{L_{total} - \sum_{i=1}^{n} L_{eff\_i}}{L_{total}}$$

Agenda

- Motivation
- Materials and Methods
  - Sample Preparation
  - Automated SEM and void analysis
- **Results**
  - Cross-section SEM micrographs
  - Individual and total void analysis
- Discussion
- Conclusion and Outlook

Results
Cross-section SEM micrographs

- Initial
  - Oval-shaped voids with similar size
  - Distributed along the bond line
- After 250 cycles
  - Voids migrate and agglomerate along Ag/Ag interface
  - Decrease in number
- After 500 cycles
  - Larger proportion of small, regular elliptical voids
  - Few large, irregularly shaped voids

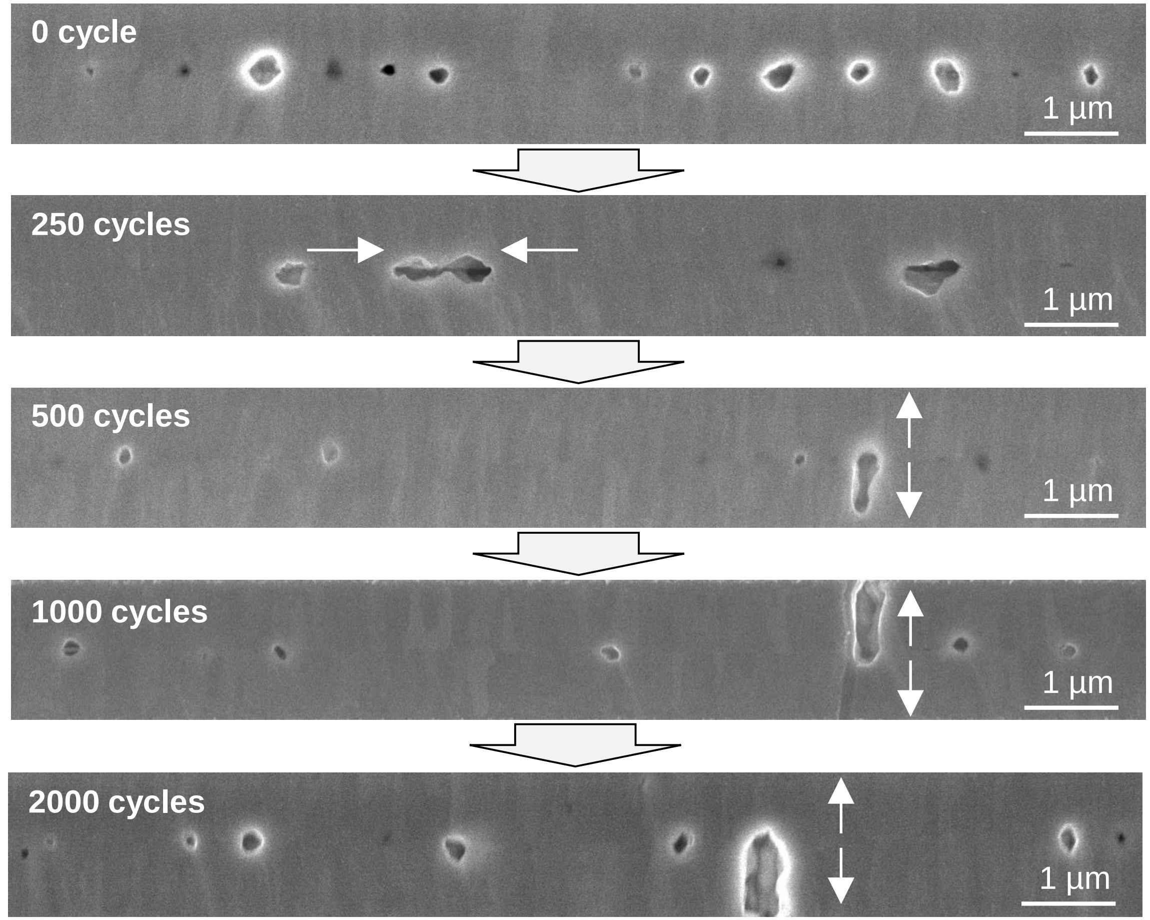

Results
Void Distribution

- x-axis: x-coordinate of individual void
- y-axis: void distance to bond line
- Size: individual void area

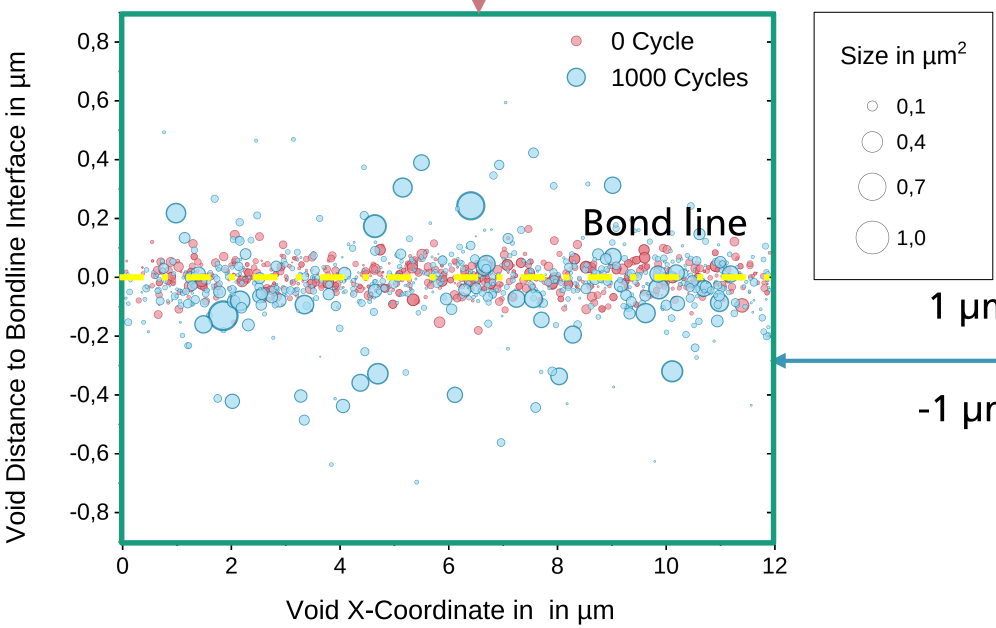

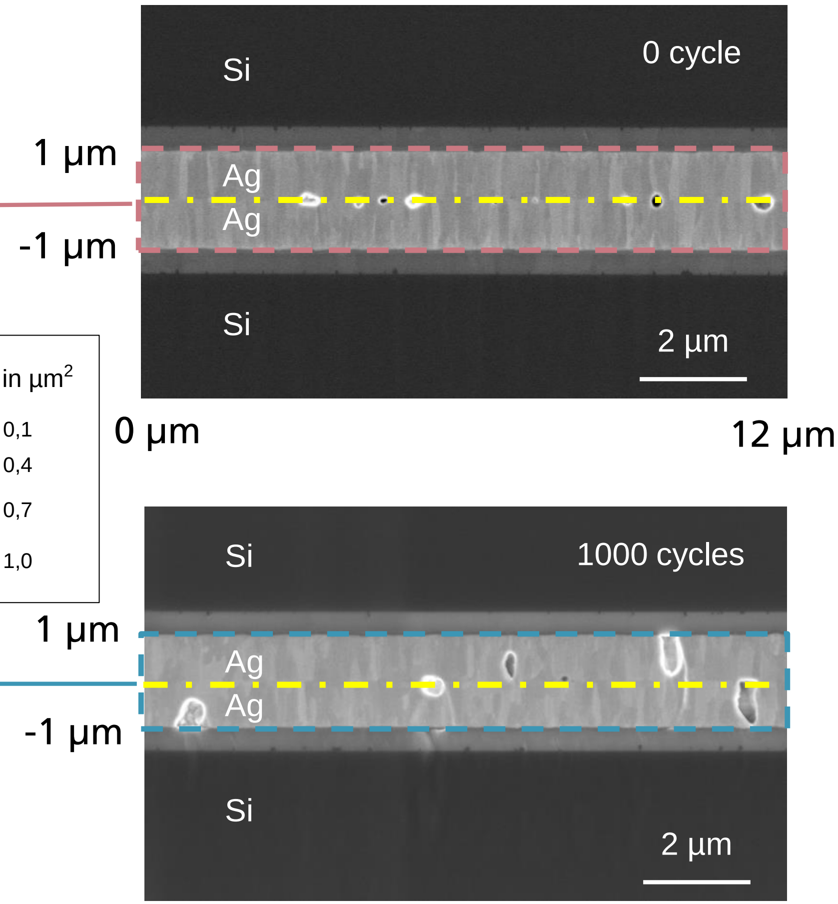

Results
Void Distribution

- Initial
  - Relativ small voids (~0.04 µm²) located close to the bonding interface
- After 250 cycles
  - Noticeable increase in void size (~0.11 µm²), still located close to the bond line

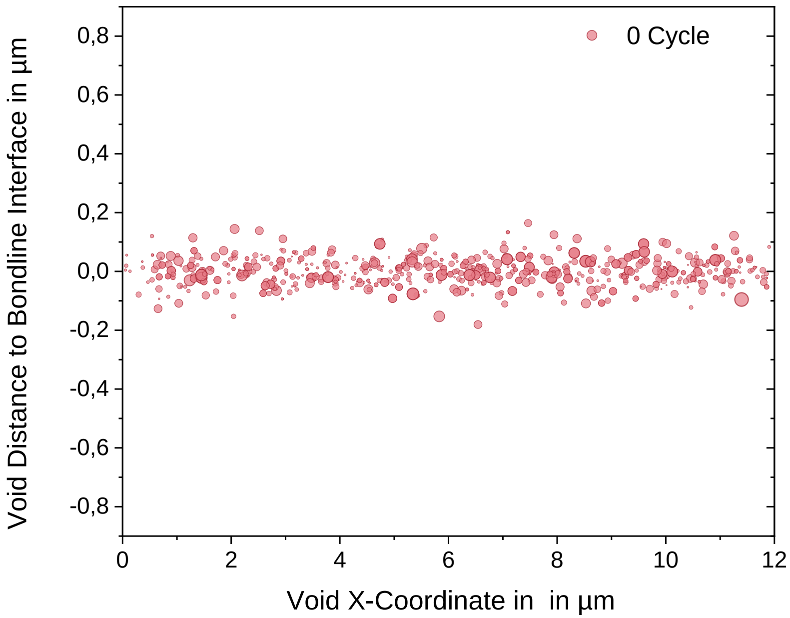

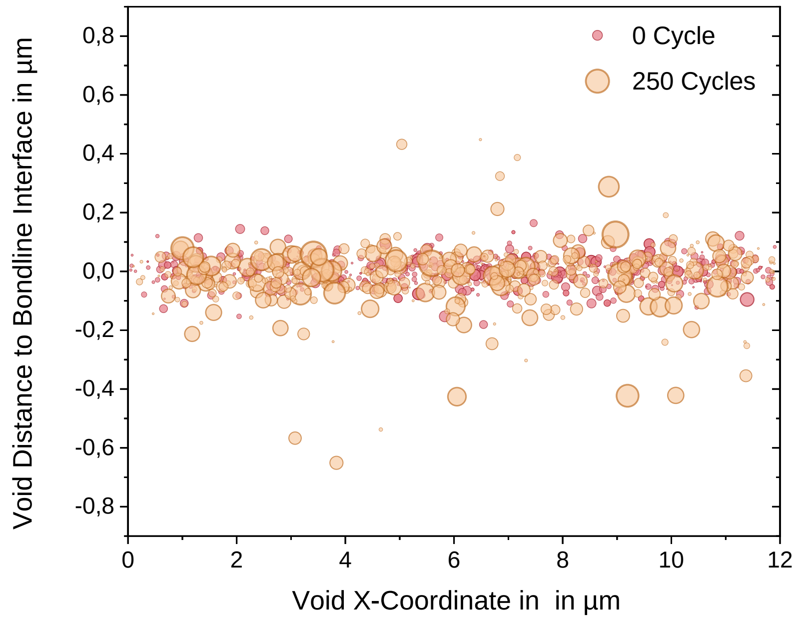

ESREF 2021

Fraunhofer IISB

Results
Void Distribution

- After 500 cycles
  - Majority of voids shrink compared to the previous stage
  - Few large voids migrating away from the bond line interface
- After 1000 cycles
  - Large voids continually increasing in number and longitudinal offset distance

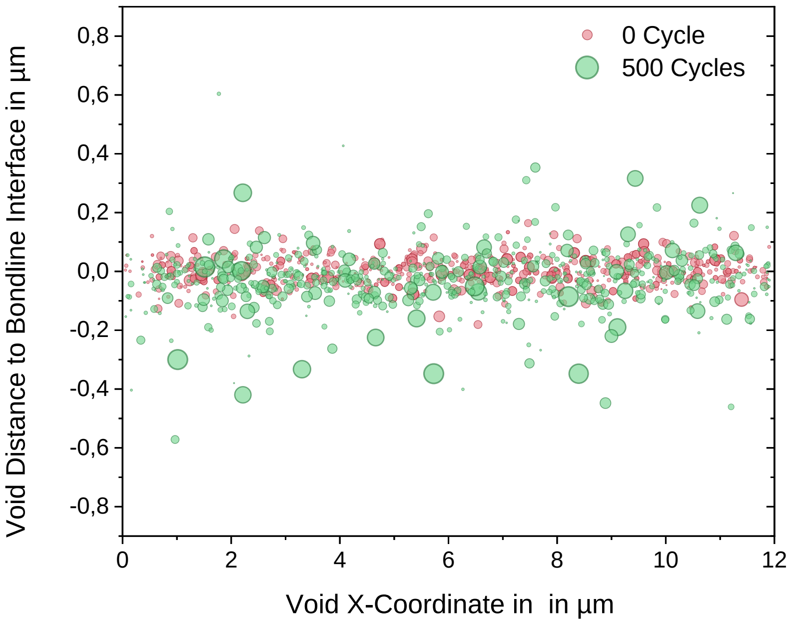

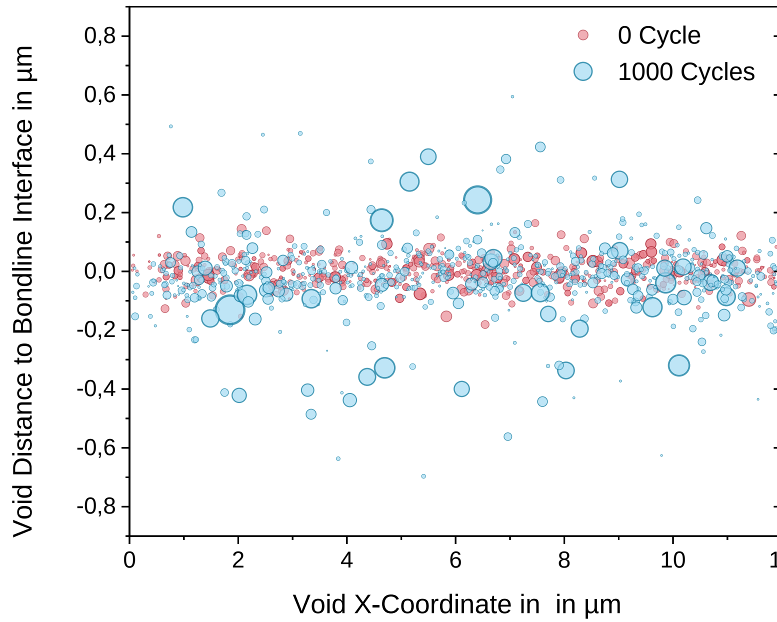

Results
Void Distribution

- After 2000 cycles
  - Following the same trend as after 500 and 1000 cycles
  - Greater number of large voids (~0.38 µm²) with an increased shift
  - Smaller-sized voids show slighter drift away from the bond line

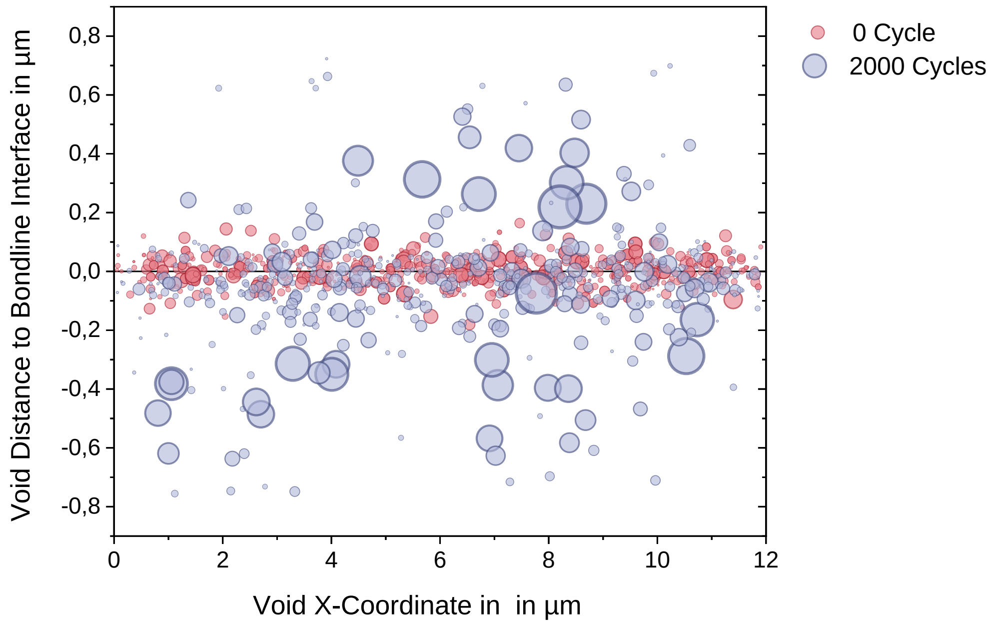

Results
Individual Void Area

- Median void area show double increase from 0.03 µm² to 0.07 µm² after 250 cycles and drops back to 0.03 µm² after 500 cycles, remains almost constant between 500 and 2000 cycles
- Outliers (about 5-10 times the initial void size) are gradually increasing with the number of TST cycles

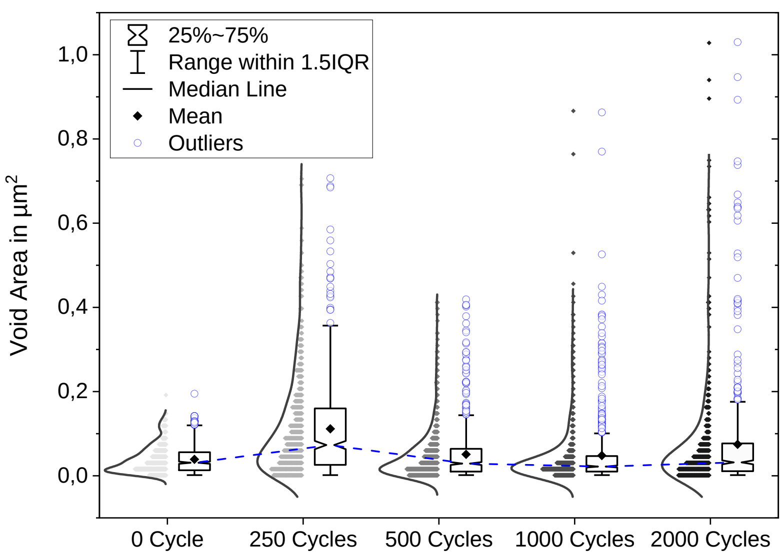

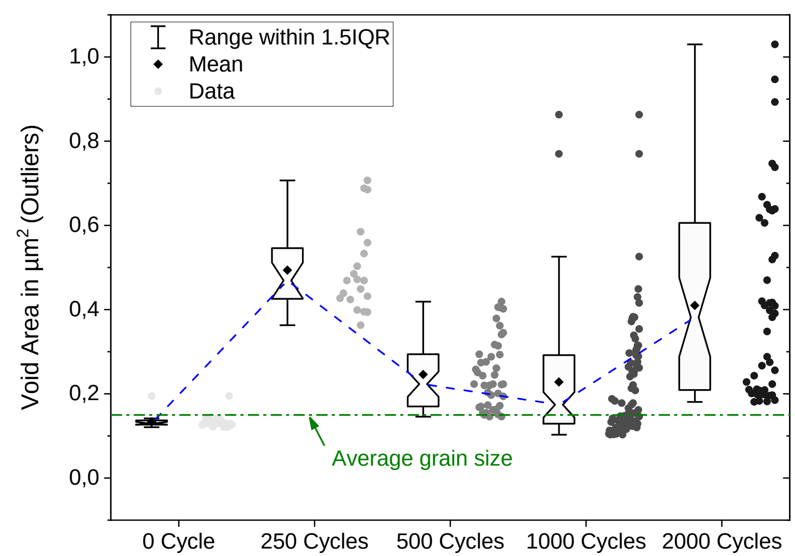

Results

Angle of Major Axis & Aspect Ratio

I. Initial:
Void major-axis orientation is nearly randomly distributed with a small aspect ratio

II. After 250 cycles:
Marked increase in aspect ratio while major axis of voids is parallel to the bond line

III. After 500/1000/2000 cycles:

- Majority of the voids have returned to a regular elliptical shape
- Some voids begin to grow in the direction perpendicular to the bonding interface

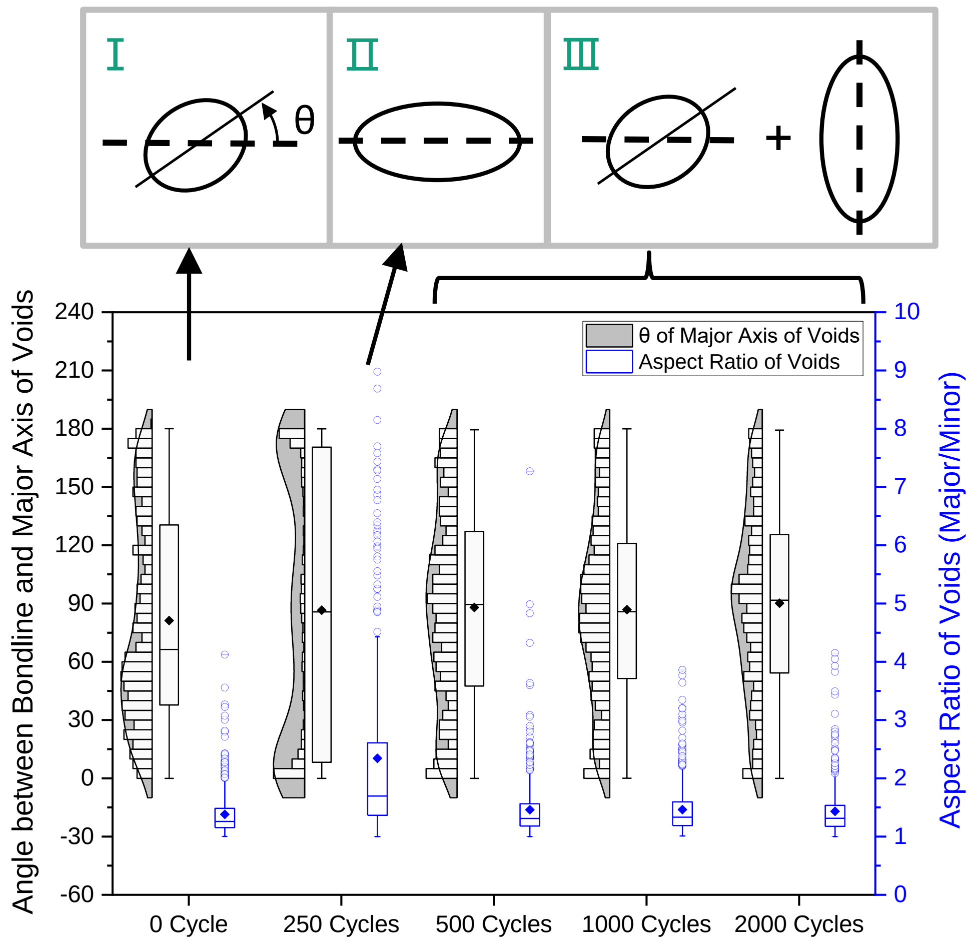

Results
Total Void Area & Counts

- Total void area rises rapidly after 250 thermal cycles, then varies only slightly upwards between 500 and 2000 cycles compared to the initial state
- Number of voids per image has decreased from 6 to less than 4 after 250 cycles and remains in a range of 4-5 up to 2000 cycles

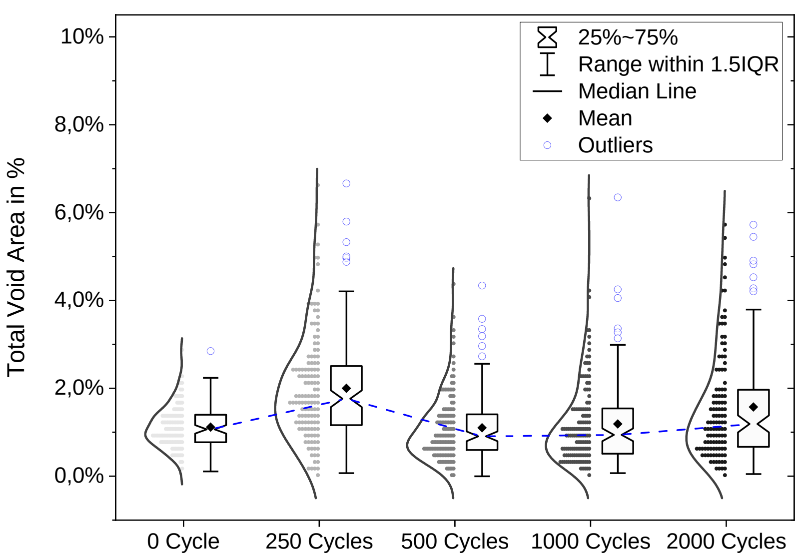

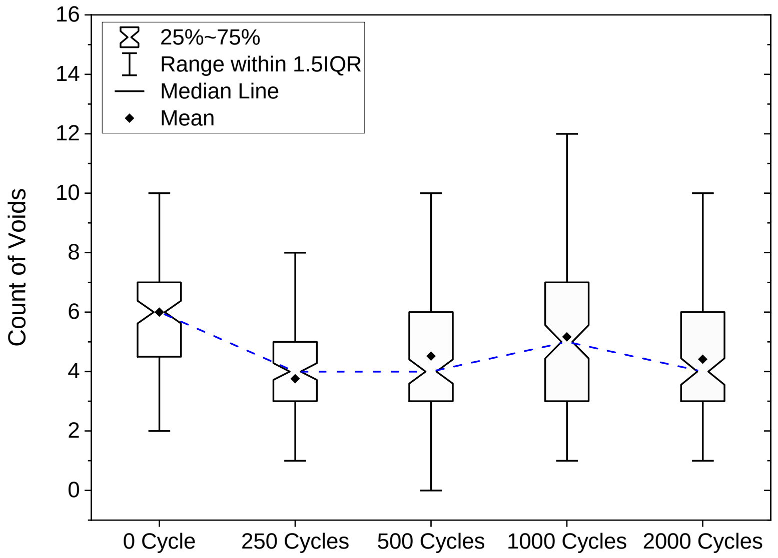

ESREF 2021
Fraunhofer IISB

Results

Bonding Ratio (%)

- Bonding ratio increases with the number of TST cycles → Ag-Ag joint interface becomes denser
- Effective bonding ratio remains almost constant
- Progressively larger gap between these two values → migration of voids away from the bond line interface

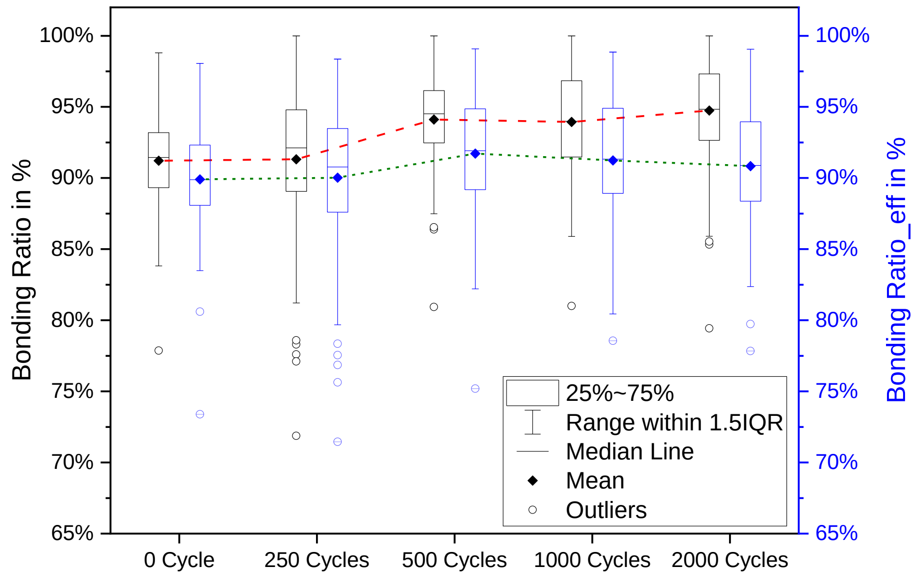

Agenda

- Motivation
- Materials and Methods
  - Sample Preparation
  - Automated SEM and void analysis
- Results
  - Cross-section SEM micrographs
  - Individual and total void analysis
- **Discussion**
- **Conclusion and Outlook**

Discussion

I. Voids are first subjected to a stress gradient along the interface → void diffusion and agglomeration along the bond line

II. After voids are collapsed, the number of voids decreases and the distance between them increases → stresses are redistributed and stress gradient at the interface decreases

III. Increase in stress gradient perpendicular to the bonding interface, which is generated due to the CTE-mismatch between metallization and silicon → voids migrate up and down in the direction away from the bond line

IV. Smaller isolated voids will gradually disappear under the influence of the accumulated compressive stresses → further reduction of the stress gradient at the bonding interface
Large voids will continue to grow and reach the Ag/barrier interface → adhesion problems or reliability issues

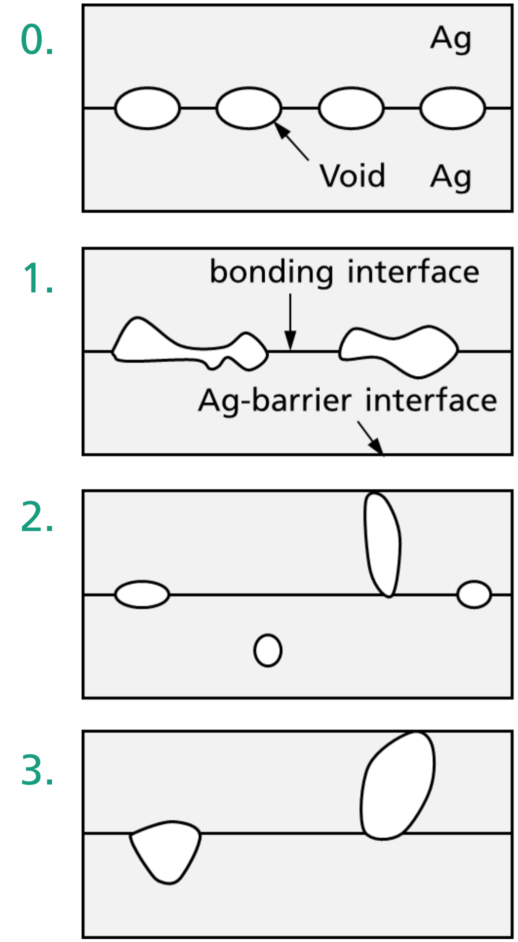

Conclusion and Outlook

- A statistical approach using a machine learning-based image classification tool was presented to analyse interfacial void morphology evolution in direct bonded Ag joints.
- The void statistics (distribution, size, shape, count, etc.) during TST have been successfully extracted from a series of SEM images.
- From the results presented, the voids are first subjected to a stress gradient along the interface, resulting in diffusion and agglomeration along the bond line. They are then driven to migrate toward the silicon substrate by the stress gradient perpendicular to the bonding interface
  → The Ag-Ag bonding interface becomes denser after 2000 TST cycles.
- The feasibility of this automated recognition and segmentation method for tracking the void morphology evolution during accelerated aging was proven.
- Outlook:
  - Validation and further optimization of this method
  - Correlation of the void microstructure information with the mechanical, thermal and electrical properties of the bonded joints

ESREF 2021
Fraunhofer IISB

References

[1] D. Hiner et al., "Multi-die chip on wafer thermo-compression bonding using non-conductive film," 2015 IEEE 65th Electronic Components and Technology Conference (ECTC), San Diego, CA, 2015, pp. 17-21.

[2] Yang, Y. et al, “Low Temperature Cu–Cu Direct Bonding Using Pillar-Concave Structure in Advanced 3D Heterogeneous Integration,” IEEE Trans. Compon., Packag. Manuf. Technol., 7(9), pp. 1560–1566.

[3] N. Rouger et al., "3D Packaging for vertical power devices," CIPS 2014; 8th International Conference on Integrated Power Electronics Systems, Nuremberg, Germany, 2014, pp. 1-6.

[4] D. E. Clark, et al (2012) Diffusion Welding of Alloys for Molten Salt Service

[5] Hill A, Wallach E (1989) Modelling solid-state diffusion bonding. Acta Metall 37(9):2425–2437

[6]Arganda-Carreras I, Kaynig V, Rueden C, Eliceiri KW, Schindelin J, Cardona A and Seung HS (2017) Trainable Weka segmentation: A machine learning tool for microscopy pixel classification. Bioinformatics 33 (15), 2424–2426.

[7] Hall, M. et al. (2009) The weka data mining software: an update. ACM SIGKDD Explor. Newslett., 11, 10–18.

THANK YOU FOR YOUR ATTENTION!

Fraunhofer IISB

Schottkystraße 10
91058 Erlangen
Germany

Zechun Yu
Zechun.yu@iisb.fraunhofer.de

www.iisb.fraunhofer.de

Contact